Design of Dimensionally Stable Composites by Evolutionary Optimization

Rodolphe Le Riche[†], Jocelyn Gaudin[†,‡]

[†] Ecole Nationale Supérieure des Mines de Paris,
Centre des Matériaux, B.P. 87 – URA CNRS 860
91003 Evry Cedex, FRANCE
e-mail: {*leriche,gaudin*}*@mat.ensmp.fr*

[‡] Aerospatiale Centre de Recherche Louis Blériot,
Département Matériaux, 12 rue Pasteur BP 76 – 92152 Suresnes Cedex, FRANCE

Abstract

The problem of designing stable composite plates is considered. In a first step, in-plane design of composite plates for high stiffness, low thermal and moisture expansion is performed. It is shown that $[(\pm\theta_1)p/(\pm\theta_2)q]_s$ stacking sequences are sufficient for in-plane design. An expert enumerative algorithm is coupled with an evolutionary search to obtain optimal plates for the in-plane problem. In a second step, a Monte Carlo laminate analysis is introduced, i.e., material and geometrical properties are distributed around their nominal value. Implications of properties distributions on the optimal design are discussed. Under the effect of properties variations, the coefficients of thermal and hygral bending of optimal in-plane designs can take on substantial values. Variations in coefficients of thermal and hygral bending are minimized by changing the laminate stacking sequence. This paper offers a unified approach to reliably designing stable composites. Design applications are given for an organic and a metal matrix composite.

1 Introduction

Dimensional stability is an increasingly important feature of space structures like telescopes, antennas, and optical plateforms. Space structure material requirements include low density, high stiffness, high micro-yield stress, low coefficients of thermal expansion, and low coefficients of moisture expansion for long term dimensional stability. Composite materials with carbon fibers supported by a light matrix can match these requirements and organic matrix composites already have a long history of applications in space[1,2]. The deterministic calculation of composite laminates has been approached at the macroscopic, mesoscopic, and microscopic scales. At a macromechanical level, the analysis of dilatation effects was proposed in the framework of the Classical Lamination Theory by Jones[3]. A micromechanical view on hygral and thermal effects has been described by Chamis[4]. The coefficient of thermal expansion was predicted by Bowles *et al.*[5] for unidirectional composites by analytical and finite element methods. Laminates with almost null coefficients of thermal expansion were derived by Ishikawa *et al.*[6] using laminate thermo-elastic invariants. However, due to manufacturing inaccuracies and variations in basic material properties, real characteristics of composites are distributed around their theoritical values. Recent interest has focused on techniques to account for the scatter in material properties. Based on given distributions of the fiber volume fraction, ply thicknesses, ply angles, fiber and matrix properties, statistical methods to estimate laminate property distributions were introduced[7,8]. Laminate distributions then need to be included in the design process, by considering not only the nominal properties, but also the associated standard deviations.

Optimizing composite structures is difficult because composite problems generally exhibit multiple local optima, and discrete variables are frequent. "Evolutionary" (also called "genetic") optimizers are stochastic search algorithms inspired from natural population genetics [9,10,11]. Because they can escape local optima and do not need gradients, evolutionary algorithms are particularly suited to composite design problems[12,13].

The purpose of the present work is to offer a unified approach to designing composite laminates accounting for thermal, hygral, and mechanical constraints. In the first part of this work, in-plane design of symmetric and balanced plates is considered. The analysis is deterministic. It is shown that the family of laminates $[(\pm\theta_1)p/(\pm\theta_2)q]_s$ covers all possible solutions to this problem. In-plane design is then performed using a coupled evolutionary and heuristic algorithm. The heuristic is in charge of varying laminate thickness, while the evolutionary algorithm optimizes ply angles. The reliability of in-plane designs are then estimated by a Monte Carlo analysis based on material and geometric properties distributions. A second optimization is performed on the stacking sequence in order to minimize the sensitivity of the laminates to basic ingredients inaccuracies. The combinatorial problem of finding the best stacking sequence at given ply angles and number of plies is addressed using a second evolutionary algorithm. Results are presented for organic as well as metal matrix composites.

2 Composite Plate Analysis

2.1 Classical Lamination Theory

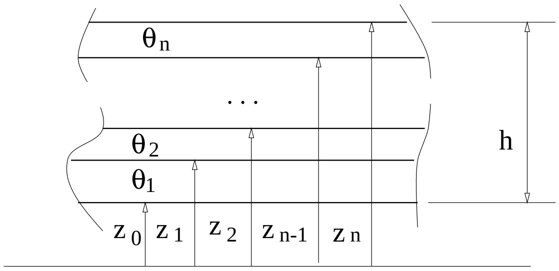

Figure 1: Laminate Conventions

Classical Lamination Theory[3] is used to calculate laminate properties, i.e., we apply Kirchhoff plate theory, and neglect through-the-thickness stresses and strains. Under those conditions, the forces $\mathbf{N}$ and moments $\mathbf{M}$ per unit length of the cross section acting on a laminate are linked to the strains ε and curvatures κ through,

$$\left\{ \begin{array}{c} \mathbf{N} \\ \mathbf{M} \end{array} \right\} = \left\{ \begin{array}{c} (N_x\ N_y\ N_{xy})^T \\ (M_x\ M_y\ M_{xy})^T \end{array} \right\} = \left[\begin{array}{cc} \mathbf{A} & \mathbf{B} \\ \mathbf{B} & \mathbf{D} \end{array} \right] \left\{ \begin{array}{c} \varepsilon \\ \kappa \end{array} \right\} = \left[\begin{array}{cc} \mathbf{A} & \mathbf{B} \\ \mathbf{B} & \mathbf{D} \end{array} \right] \left\{ \begin{array}{c} (\varepsilon_x\ \varepsilon_y\ \varepsilon_{xy})^T \\ (\kappa_x\ \kappa_y\ \kappa_{xy})^T \end{array} \right\} . \quad (1)$$

The coefficients of the 3×3 extensional, coupling and flexural stiffness matrices, $\mathbf{A}$, $\mathbf{B}$, $\mathbf{D}$, respectively, are functions of the material properties, the fiber orientations in each ply, and the position and number of ply interfaces z_i (cf. Figure 1). For an n plies laminate, the total laminate thickness is $h = z_n - z_0$. In this study, the analysis is carried out for general laminates, therefore the $\mathbf{A}$, $\mathbf{B}$, and $\mathbf{D}$ matrices are filled. The stiffness matrix of equation (1) can be inverted and yields the laminate compliance matrix,

$$\left[\begin{array}{cc} A & B \\ B & D \end{array} \right]^{-1} = \left[\begin{array}{cc} a & b \\ b^T & d \end{array} \right] . \quad (2)$$

The effective Young's moduli of the laminate in the longitudinal, and transverse direction, E_x, E_y, and shear modulus G_{xy}, respectively, are expressed as,

$$E_x = \frac{a_{11}}{h} \quad , \quad E_y = \frac{a_{22}}{h} \quad , \quad G_{xy} = \frac{a_{66}}{h} \ , \tag{3}$$

where the index 6 points to the third row/column of the relevant matrix.

For a laminate under general loading conditions, the forces and moments result from the superposition of the mechanical, thermal, and hygral forces and moments, $\mathbf{N}^m$, $\mathbf{N}^T$, $\mathbf{N}^H$, $\mathbf{M}^m$, $\mathbf{M}^T$, and $\mathbf{M}^H$, respectively. Decomposing the loads in equation (1) yields,

$$\left\{ \begin{array}{c} \varepsilon \\ \kappa \end{array} \right\} = \left[\begin{array}{cc} a & b \\ b^T & d \end{array} \right] \left\{ \begin{array}{c} N^m + N^T + N^H \\ M^m + M^T + M^H \end{array} \right\} \ . \tag{4}$$

The thermal and hygral forces and moments are defined as[3],

$$\mathbf{N}^T = \sum_{k=1}^{n} \bar{\mathbf{Q}}_k \bar{\alpha}_k^T (z_k - z_{k-1}) \Delta T \quad , \quad \mathbf{M}^T = \frac{1}{2} \sum_{k=1}^{n} \bar{\mathbf{Q}}_k \bar{\alpha}_k^T (z_k - z_{k-1})^2 \Delta T \quad , \tag{5}$$

$$\mathbf{N}^H = \sum_{k=1}^{n} \bar{\mathbf{Q}}_k \bar{\alpha}_k^H (z_k - z_{k-1}) \Delta H \quad , \quad \mathbf{M}^H = \frac{1}{2} \sum_{k=1}^{n} \bar{\mathbf{Q}}_k \bar{\alpha}_k^H (z_k - z_{k-1})^2 \Delta H \quad , \tag{6}$$

where $\bar{\mathbf{Q}}$ is the reduced ply stiffness matrix in laminate coordinates, and $\bar{\alpha}^T$ and $\bar{\alpha}^H$ are the ply coefficients of thermal and hygral expansion in the laminate coordinates, respectively. ΔT is the temperature variation and ΔH is the moisture variation. The strains and curvatures obtained from equation (4) when $\mathbf{N}^m = \mathbf{M}^m = \mathbf{N}^H = \mathbf{M}^H = 0$ and $\Delta T = 1°$ are the coefficients of thermal expansion (CTE) and curvature, α^T and $\mathbf{W}^T$. Identically, when mechanical and thermal loads are set to zero and $\Delta H = 1$ %M, the strains and curvatures of equation 4 are the coefficients of moisture expansion (CME) and bending α^H (or more commonly β) and $\mathbf{W}^H$.

2.2 Two Angles for In-plane Design

We now assume that the laminate is symmetric and balanced, which induces that $\mathbf{B} = 0$, and $A_{16} = A_{26} = 0$. The in-plane and out-of-plane behaviors are thus decoupled. Considering exclusively in-plane behavior, the constitutive equations of the laminate are,

$$\left\{ \begin{array}{c} N_x^m + N_x^T + N_x^H \\ N_y^m + N_y^T + N_y^H \\ N_{xy}^m + N_{xy}^T + N_{xy}^H \end{array} \right\} = \left[\begin{array}{ccc} A_{11} & A_{12} & 0 \\ A_{12} & A_{22} & 0 \\ 0 & 0 & A_{66} \end{array} \right] \left\{ \begin{array}{c} \varepsilon_x \\ \varepsilon_y \\ \gamma_{xy} \end{array} \right\} \ . \tag{7}$$

The coefficients of the $\mathbf{A}$ matrix can be expressed as (which also stands for unsymmetric or unbalanced laminates),

$$\begin{array}{rcl} A_{11} &=& U_1 h + U_2 V_1 + U_3 V_3 \quad , \\ A_{12} &=& U_4 h - U_3 V_3 \quad , \\ A_{22} &=& U_1 h - U_2 V_1 + U_3 V_3 \quad , \\ A_{66} &=& U_5 h - U_3 V_3 \quad . \end{array} \tag{8}$$

The scalars U_1 to U_5 are the material invariants. They depend only on the unidirectional material properties. The material invariants are defined as,

$$\begin{array}{rcl} U_1 &=& \frac{1}{8}(3Q_{11} + 3Q_{22} + 2Q_{12} + 4Q_{66}) \quad , \\ U_2 &=& \frac{1}{2}(Q_{11} - Q_{22}) \quad , \\ U_3 &=& \frac{1}{8}(Q_{11} + Q_{22} - 2Q_{12} - 4Q_{66}) \quad , \\ U_4 &=& \frac{1}{8}(Q_{11} + Q_{22} + 6Q_{12} - 4Q_{66}) \quad , \\ U_5 &=& \frac{1}{8}(Q_{11} + Q_{22} - 2Q_{12} + 4Q_{66}) \quad . \end{array} \tag{9}$$

The two parameters V_1 and V_3 in equation (8) reflect only the inluence of the stacking sequence. These lamination parameters are defined as[14],

$$V_1 = \int_{-h/2}^{h/2} \cos 2\theta dz \quad , \quad V_3 = \int_{-h/2}^{h/2} \cos 4\theta dz \quad . \tag{10}$$

Equations (7) to (10) imply that $\mathbf{A}$, thus $\mathbf{a}$, E_x, E_y, E_{xy}, ε_x, ε_y, and γ_{xy}, are related to the stacking sequence through two parameters, V_1 and V_3.

We now consider dilatation effects on the design of laminates. The load stemming from dilatation was expressed as (equation (6)),

$$N^d = \int_{-h/2}^{h/2} \bar{\mathbf{Q}}\bar{\alpha}^d dz = \sum_{k=1}^{n} \bar{\mathbf{Q}}_k \bar{\alpha}_k^d (z_{k-1} - z_k)\Delta d \quad , \quad d = H, T \ , \tag{11}$$

where d accounts for either thermal or hygral effects[1]. Equation (11) can be rewritten in terms of the dilato-elastic invariants[6] U_1^d and U_2^d, for general laminates,

$$\left\{ \begin{array}{c} N_x^d \\ N_y^d \\ N_{xy}^d \end{array} \right\} = \frac{1}{2} \left\{ \begin{array}{c} U_1^d + U_2^d V_1 \\ U_1^d - U_2^d V_1 \\ U_2^d V_2 \end{array} \right\} \quad , \tag{12}$$

where $V_2 = \int_{-h/2}^{h/2} \sin 2\theta dz$. If the laminate is balanced, $V_2 = 0$, and $N_{xy}^d = 0$. The dilato-elastic invariants U_1^d and U_2^d are calculated as,

$$\begin{array}{rcl} U_1^d &=& Q_{11}\alpha_{\mathcal{L}}^d + Q_{12}(\alpha_{\mathcal{T}}^d + \alpha_{\mathcal{L}}^d) + Q_{22}\alpha_{\mathcal{T}}^d \quad , \\ U_2^d &=& Q_{11}\alpha_{\mathcal{L}}^d + Q_{12}(\alpha_{\mathcal{T}}^d - \alpha_{\mathcal{L}}^d) - Q_{22}\alpha_{\mathcal{T}}^d \quad , \end{array} \tag{13}$$

where $\alpha_{\mathcal{L}}^d$ and $\alpha_{\mathcal{T}}^d$ are the longitudinal and transverse coefficients of expansion, respectively. From equations (7) and (12), the in-plane coefficients of thermal and hygral expansion are obtained by,

$$\left\{ \begin{array}{c} \alpha_x^T \\ \alpha_y^T \\ \alpha_{xy}^T \end{array} \right\} = \frac{1}{2}[\mathbf{a}] \left\{ \begin{array}{c} U_1^T + U_2^T V_1 \\ U_1^T - U_2^T V_1 \\ 0 \end{array} \right\} \quad \text{, and} \quad \left\{ \begin{array}{c} \beta_x \\ \beta_y \\ \beta_{xy} \end{array} \right\} = \frac{1}{2}[\mathbf{a}] \left\{ \begin{array}{c} U_1^H + U_2^H V_1 \\ U_1^H - U_2^H V_1 \\ 0 \end{array} \right\} \quad . \tag{14}$$

With respect to stacking sequences, those coefficients depend only on the parameters V_1 and V_3 (in $\mathbf{a}$). Globally, all in-plane mechanical, thermal, and hygral laminate properties are influenced by the stacking sequence through two lamination parameters, V_1 and V_3. Two continuous angles θ_1 and θ_2 are sufficient to describe all possible combinations of V_1 and V_3 if the proportion of θ_1 and θ_2 plies is well chosen. Therefore, a general stacking sequence for in-plane design of laminates accounting for mechanical, thermal, and hygral properties is $((\pm\theta_1)_{n_1/2}/(\pm\theta_2)_{n_2/2})_s$.

2.3 Micromechanical Analysis

Including micromechanical relations in our analysis permits studying the effect of fibre and matrix properties changes, first on the ply properties, and next on laminate properties. Ply hygral, thermal, and mechanical properties are calculated from micromechanical data according to the relations given in [4], where the fibers are assumed to be transversly isotropic. Denoting by the indices $\mathcal{L}$ and $\mathcal{T}$ the

[1] α^H, the coefficients of hygral expansion is usually known as β. α^d is used only in this section to avoid redundant equations. After this section, α^T will be denoted α, and α^H, β.

longitudinal and transverse directions, by V_f the fiber volume fraction, and by f and m fiber and matrix properties, respectively, the micro-meso relationships are,

$$\rho = V_f \rho_f + (1 - V_f)\rho_m \quad , \tag{15}$$

$$E_{\mathcal{L}} = V_f E_{\mathcal{L},f} + (1 - V_f) E_m \quad , \tag{16}$$

$$E_{\mathcal{T}} = \frac{E_m}{1 - \sqrt{V_f}(1 - E_m / E_{\mathcal{T},f})} \quad , \tag{17}$$

$$G_{\mathcal{LT}} = \frac{G_m}{1 - \sqrt{V_f}(1 - G_m / G_{\mathcal{LT},f})} \quad , \tag{18}$$

$$\nu_{\mathcal{LT}} = V_f \nu_{\mathcal{LT},f} + (1 - V_f)\nu_m \quad , \tag{19}$$

$$\alpha_{\mathcal{L}}^T = \frac{V_f \alpha_{\mathcal{L},f}^T E_{\mathcal{L},f} + (1 - V_f)\alpha_m^T E_m}{E_{\mathcal{L}}} \quad , \tag{20}$$

$$\alpha_{\mathcal{T}}^T = \alpha_{\mathcal{T},f}^T \sqrt{V_f} + (1 - \sqrt{V_f})(1 + V_f \nu_m E_{\mathcal{L},f} / E_{\mathcal{L}})\alpha_m^T \quad , \tag{21}$$

$$\beta_{\mathcal{L}} = \frac{(1 - V_f)\alpha_m^H E_m}{E_{\mathcal{L}}} \quad , \tag{22}$$

$$\beta_{\mathcal{T}} = \alpha_m^H (1 - \sqrt{V_f})(1 + \sqrt{V_f} \frac{(1 - \sqrt{V_f})E_m}{\sqrt{V_f} E_{\mathcal{T}} + (1 - \sqrt{V_f})E_m}) \quad . \tag{23}$$

2.4 Monte Carlo Analysis

In practice, the basic laminate components vary due to manufacturing uncertainties. Those uncertainties can be accounted for using a Monte Carlo analysis of the laminate.

In the Monte Carlo analysis, basic laminate components are supposed to be normal random variables. Each variable is associated to an average, the nominal variable value, and a standard deviation. Fiber volume fraction, fiber and matrix moduli and coefficients of dilatation vary from one laminate to another. Fiber orientations and ply thicknesses vary independently between plies. As a result of the basic laminate properties being random variables, the laminate mechanical properties (laminate effective Young's moduli, stiffness matrices, coefficients of thermal and hygral expansion) are also random variables. The average $\bar{P}$ and standard deviation $\sigma(P)$ of the laminate macromechanical properties P are estimated using n_{MC} trials of the laminate micromechanical properties and laminate specifications.

It is important to include statistical characteristics of the laminate properties in the design procedure. An optimization that neglects the distribution of properties risks producing unsatisfactory or unreliable designs. For example, because of imprecisions in the fiber angles, real laminates will never be exactly symmetrical, i.e., they will bend when the external temperature and hygrometry change. The optimization described in Section 3.5 is an attempt to control this phenomenon.

3 Optimization Problem Formulation

3.1 Designing for Dimensional Stability

The present work is primarily meant for space structural design, where dimensional stability is a stringent requirement. Generally, motivations for dimensionally stable design are the following:

- The final structure should be as light as possible.
- High stiffness is required to avoid vibration mode couplings between the launcher and the structure.
- High micro-yield stress is required. Micro-yield stress is the stress that induces a residual strain of 10^{-6} in the material. This property cannot be calculated by a simple law and depends on

many parameters, but it is generally accepted that for carbon fiber composites, disorienting plies with respect to the load trajectory decreases the micro-yield stress. For a given composite, the smaller the strain at maximum load, the smaller the residual strain when the load is suppressed. Because of these arguments, in a first approximation, the micro-yield stress criterion is implicitely implemented through a strain and a stiffness criterion.

- The coefficient of thermal expansion, α, should be small. In space, satellites endure large temperature variations. Even if temperature changes can be reduced by thermal control, they are never completely suppressed. To avoid large strains during thermal cycles, α is kept as low as possible.

- Dimensions should be stable through time. Moisture desorption and stress relaxation are the dominant phenomena that modify the length of aging structure parts. Some materials, such as organic matrices, tend to absorb moisture on earth and desorb it in space. This desorption implies a change in length of the material, according to its coefficient of moisture expansion, β. Because completely dried out composites are very difficult to obtain, the minimization of β is a practical way of reducing temporal dimensional instabilities. Dimensional variations due to stress relaxation are not considered here.

- Reproductibility is important for high dimensional stability applications. It depends on manufacturing techniques control and on basic materials properties dispersion. Composite sensitivity to ingredients properties dispersions has to be kept as low as possible.

3.2 Problem Decomposition

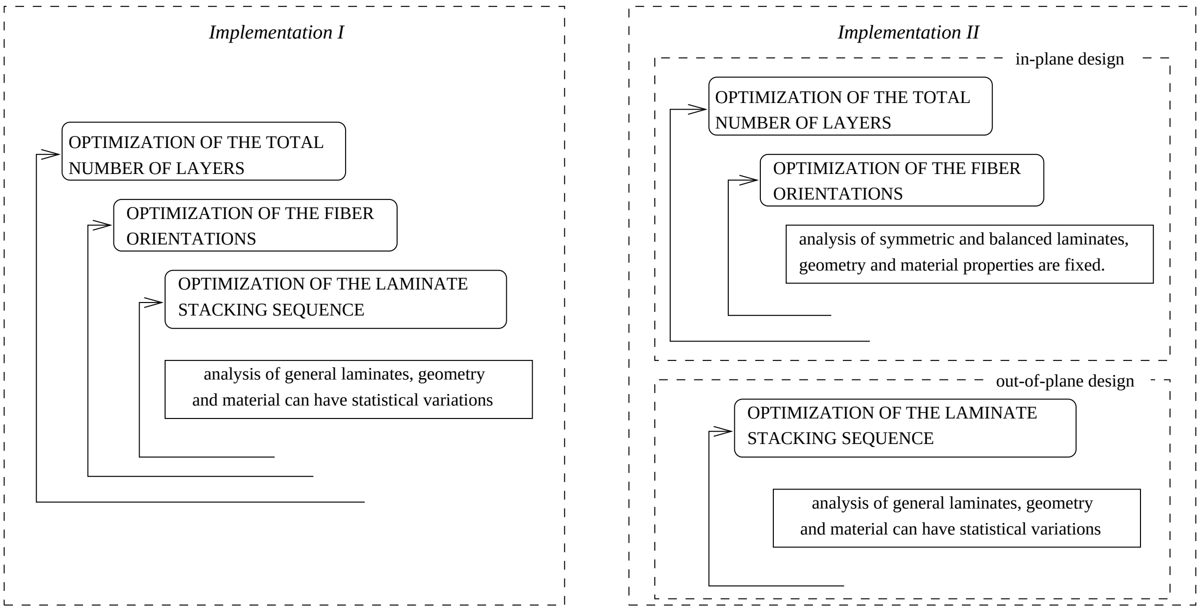

Figure 2: Decomposition of the Optimization Problem

A design procedure is proposed to find the lightest, most stable laminated plate that achieves mechanical requirements. Variations in the laminate composition due to manufacturing uncertainties are accounted for.

The global optimization is divided into three dependent subproblems: the minimization of the laminate total number of layers, the determination of the fiber orientations inside each layer, and the stacking arrangement of the plies (at given ply orientations). Three strategies are implemented to treat the thickness, ply orientation, and stacking sequence optimizations. Figure 2 shows two different ways of interlocking the three levels of laminate design. A global optimization procedure would result from the arrangement *I*. The outermost loop changes the number of layers, then, for a given total thickness, the angles are chosen while the stacking sequence is optimized for each given set of angles. However, implementation *I* has a dauntingly high numerical cost: of the order of 10 min. CPU on a SUN SparcStation 20-612 were needed to carry out a single Monte Carlo analysis of a laminate ($n_{MC} = 10000$ laminates evaluated). If we first consider symmetric and balanced laminates, with deterministic properties, in-plane laminate design no longer involves the stacking sequence. In this case, the optimization can be decomposed as shown in Figure 2-*II*. In implementation *II*, the in-plane design step determines the number of layers and the ply orientations. Next, out-of-plane optimization minimizes effects of manufacturing uncertainties by varying the stacking sequence. Such a decomposition of the in-plane and out-of-plane designs is motivated by the fact that $\mathbf{W}^d$, the bending coefficient of dilatation, is the laminate characteristic that changes the most with manufacturing errors, and it is efficiently controlled by the stacking sequence. Examples are given in Section 5. Implementation *II* permits designing stable composite laminates at a low numerical cost, it is therefore applied in this work.

3.3 Thickness Optimization

Thickness optimization is the outermost loop of the in-plane design process. In-plane optimization takes place for different values of the fiber volume fraction, V_f. A lower bound on the fiber volume fraction stems from the smallest admissible value of the the longitudinal modulus E_x. Indeed, the largest value of E_x is obtained with a unidirectional laminate (or UD, all fibers have a 0^o orientation). If the UD does not reach the required value of E_x, E_x^{min}, it is necessary to increase the fiber volume fraction V_f. Repetition of this process yields a lower bound V_f^{min} on the fiber volume fraction V_f. Similarly, a lower bound on the total laminate thickness at a given fiber volume fraction V_f is calculated by increasing the number of layers of a UD until longitudinal strains $|\varepsilon_x|$ are below their allowable value, ε_x^{allow}. It has been seen in Section 2.2 that it is sufficient to consider sequences like $((\pm\theta_1)_{n1/2}/(\pm\theta_2)_{n2/2})_s$ for in-plane design. The lower bound on the laminate thickness applies to $(n_1 + n_2) = n/2$. Because the stacking sequence of the laminate is simple and lower bounds on V_f and $(n_1 + n_2)$ can be estimated, the design space for this subproblem has a small size. In this case, a specialized enumerative algorithm will be as efficient as an optimization algorithm. The enumerative algorithm solves the problem,

for different V_f

Minimize	$n_1 + n_2$,	(24)
by changing	n_1 and n_2 ,	
such that	there is a design that solves the fiber orientation in-plane design problem	

The enumerative algorithm for fiber fraction and thickness variation is described below:

- *while* $(E_x(UD) \ < \ E_x^{min})$ *, increase* $V_f \to V_f^{min}$.
- *for* $V_f \ = \ V_f^{min}$*, while* $|\varepsilon_x(UD)| \ > \ \varepsilon_x^{allow}$*, increase* $n \to n_{min}$
- *DO,* $V_f = V_f^{min}$*,*
  - *DO,* $n = n_{min}$*,*
    * *DO,* $n_1 = 0$*,*
      · *DO,* $n_2 = 0$*, If [(* $2(n_1 + n_2) \ = \ n$*) and (*n_1 *or* n_2 *even and* $\neq 0$*)],*
      optimize θ_1 *and* θ_2 *(cf. Section 3.4) (*θ_i*=0 if* n_i *odd,* $i = 1, 2$*)*
      $n_2 = n_2 + 1$
      · *UNTIL* $n_2 > \min(n_1, n/2 - n_1)$
      · $n_1 = n_1 + 1$
    * *UNTIL* $n_1 > n/2$
    * *if a feasible design has been found, stop.*
    * *n = n+2*
  - *UNTIL* $n \geq n_{max}$
- $V_f \ = \ V_f + \Delta V_f$
- *UNTIL* $V_f \geq V_f^{max}$

In the central optimization of the ply orientation, θ_i is set to 0 when n_i is odd because 0_{n_i} is the only possible sequence that match $(\pm\theta_i)_{n_i/2}$, $i = 1, 2$. The conditions in the enumerative algorithm guarantee that only meaningfull combinations of n_1 and n_2 are produced.

3.4 In-plane Angle Ply Optimization

Angle ply optimization takes place inside the enumeration for each candidate V_f, n_1 and n_2. The enumeration and the angle ply optimization represent the complete solution of the deterministic in-plane design problem. The ply angle in-plane design problem is formulated as,

$$\begin{array}{rl} \text{Minimize} & \dfrac{|\alpha_x^T|}{\alpha_x^{t,allow}} \quad , \\ \text{by changing} & \theta_1 \text{ and } \theta_2 \quad , \\ \text{such that} & \dfrac{E_x}{E_x^{min}} - 1 \geq 0 \quad , \quad \dfrac{E_y}{E_y^{min}} - 1 \quad , \\ & 1 - \dfrac{|\varepsilon_x|}{\varepsilon_x^{allow}} \geq 0 \quad , \quad 1 - \dfrac{|\varepsilon_y|}{\varepsilon_y^{allow}} \geq 0 \quad , \quad 1 - \dfrac{|\beta_x|}{\beta_x^{allow}} \geq 0 \quad , \end{array} \tag{25}$$

where $\alpha_x^{t,allow}$ and β_x^{allow} are allowable coefficients of thermal and hygral expansion, ε_x^{allow} and ε_y^{allow} are allowable values for the longitudinal and transverse strains, E_x^{min} and E_y^{min} are lower bounds of the longitudinal and transverse Young's moduli. The angles θ_1 and θ_2 are continuous design variables.

3.5 Stacking Sequence Optimization

The third and last part of our laminate design procedure is the determination of the stacking sequence at fixed fiber fraction volume V_f, number of plies n_1 and n_2, and fiber angles θ_1 and θ_2. Stacking sequence design accounts here for basic ingredients properties scatter: the deterministic analysis of a laminate design is replaced by a Monte Carlo analysis. Because of the perturbations of the θ_i's, the laminates are no longer symmetric and balanced. The main goal of the stacking sequence optimization is to minimize bending due to dilatation. $\mathbf{W}^d$, $d = T, H$, is a function of the stacking sequence through matrices $\mathbf{b}$ and $\mathbf{d}$ in equation (4). In-plane properties are not included in this formulation because they do not vary as drastically as bending properties. Furthermore, since the longitudinal dimension is preponderant in one of our applications, the minimization concerns W_x^d, while W_y^d and W_{xy}^d are included in the constraints. It will be shown in Section 6 that the averages of the bending dilatation coefficients, $\bar{W}_x^d$, $\bar{W}_y^d$, $\bar{W}_{xy}^d$ remain close to 0 in the Monte Carlo analysis. Therefore, the stacking sequence design problem accounts only for the standard deviations of the bending coefficients, $\sigma(W_x^d)$, $\sigma(W_y^d)$, $\sigma(W_{xy}^d)$. We seek to

$$\begin{array}{ll} \text{minimize} & \dfrac{\sigma(W_x^d)}{\sigma(W_x^{d,allow})} \ , \\ \text{by changing} & \text{the location of the plies} \ , \\ \text{such that} & 1 - \dfrac{\sigma(W_y^d)}{\sigma(W_y^{d,allow})} \geq 0 \quad , \quad 1 - \dfrac{\sigma(W_{xy}^d)}{\sigma(W_{xy}^{d,allow})} \geq 0 \ , \end{array} \tag{26}$$

where *allow* upperscript designates allowable values of the standard deviations. An alternative formulation integrates the curvatures into the deflection of a corner of the plate. This deflection f is calculated as,

$$f^d = \frac{1}{2} W_x^d \, s_L^2 + \frac{1}{2} W_y^d \, s_W^2 + \frac{1}{2} W_{xy}^d \, s_L \, s_W, \tag{27}$$

where s_L and s_W are the length and the width of the plate, respectively. The resulting stacking sequence optimization problem is,

$$\begin{array}{ll} \text{minimize} & \dfrac{\sigma(f^d)}{\sigma(f^{d,allow})} \ , \\ \text{by changing} & \text{the location of the plies} \ , \end{array} \tag{28}$$

For the stacking sequence optimization, there are 4 different angle orientations $+\theta_1$, $-\theta_1$, $+\theta_2$ and $-\theta_2$, each represented by $n_1/2$, $n_1/2$, $n_2/2$, and $n_2/2$ plies, respectively. The total number of plies in the laminate is $n = 2 \times (n_1 + n_2)$, but since the laminate is symmetric, the location of $n/2 = n_1 + n_2$ plies need to be determined. The design space size is $\begin{pmatrix} n_1 + n_2 \\ n_1/2 \end{pmatrix} \times \begin{pmatrix} n_1/2 + n_2 \\ n_1/2 \end{pmatrix} \times \begin{pmatrix} n_2 \\ n_2/2 \end{pmatrix}$. For instance, if $n_1 = n_2 = 8$, the total number of possible stacking sequences is about 218 billions.

4 Evolutionary Optimization Algorithms

The description of the enumerative algorithm for changing the fiber volume fraction and the number of plies is self-contained with the formulation of the optimization problem in Section 3.3. We now present the optimization methods used to calculate optimal values of the fiber orientations θ_1 and θ_2, and optimal stacking sequences. Both methods derive from evolutionary optimization ideas. Evolutionary optimizers are stochastic searches inspired from natural species genetics[9,10,11]. The following properties of evolutionary optimizers explain the growing popularity they have known in engineering design[11,12,15]: contrary to gradient based optimizers, they can handle non-convex optimization problems. For example, the design variables can be continuous and / or discrete. Evolutionary optimizers can also escape local optima (thanks to the random choices that intervene in the creation of new design points). Evolutionary algorithms are generally among the most efficient stochastic optimizers. Those characteristics are crucial to robustly solve composite design problems. First, the ply angle optimization problem is, in general, non-convex and has local optima. Second, finding the optimal stacking sequence is a combinatorial optimization problem, i.e., it involves discrete design variables.

Evolutionary optimizers process a set of design points, called a "population". Encoding schemes, which depend on the application, are used to represent design points. A flow chart of a "steady state" evolutionary optimizer is given in Figure 3. The initial population of design points is usually created at random. Next, the performance of those points with respect to the optimization problem is evaluated. This performance is a scalar value. In the case of a constrained optimization problem, the performance is a penalized objective function value, which is calculated as follows. The initial optimization problem with n_g inequality constraints,

$$\begin{aligned} \text{minimize} \quad & f(\mathbf{x}) \ , \\ \text{by changing} \quad & \mathbf{x} \ , \\ \text{such that} \quad & g_i(\mathbf{x}) \leq 0 \ , i = 1, n_g \ , \end{aligned} \tag{29}$$

is transformed into the penalized unconstrained optimization problem,

$$\begin{aligned} \text{minimize} \quad & f_p(\mathbf{x}) \ = \ f(\mathbf{x}) \ + \ p \max_{i=1,n_g} (0, g_i(\mathbf{x})) \ , \\ \text{by changing} \quad & \mathbf{x} \ , \end{aligned} \tag{30}$$

where p is a penalty parameter.

Once the penalized objective functions of the population have been evaluated, the points are ranked: lower objective function points have the highest rank. Next, a pair of points is selected. The probability of selection is equal to the normalized rank. For instance, the best solution so far in a population of n_{pop} points has a probability of $\{2n_{pop}/(n_{pop}(n_{pop}+1))\}$ of being selected at each trial. Selection is repeated until two different points have been chosen. The two selected points are used to produce a new design point through an operation called "crossover". Then, the new design point is transformed by a mutation operator. After the new design point has been evaluated, it replaces the worst point so far in the population. Crossover and mutation operators are application dependent. The basic idea is that crossover should mix features carried by each of the two parent points. The goal of mutation is to randomly perturb new design points, thus introducing new features in the population. Although random, mutation is necessary. Without mutation, the population of design points would rapidly become uniform under the conjugated effect of selection and crossover. Once a population has converged to a single point, crossover cannot generate new points, hence the need for mutation. The process of selection - crossover - mutation - analysis is repeated until a maximum number of points have been evaluated.

In the two next sections, we present application dependent implementations of the evolutionary optimizer (encoding scheme, crossover and mutation operators) for ply angle and stacking sequence design.

4.1 Continuous Numbers Optimization

The encoding scheme used for continuous ply angle design variables is a straightforward base 10 encoding. A ply orientation design is coded $(\theta_1 \quad \theta_2)$.

"Flat crossover"[16] is the crossover used for ply angle design. It is applied with a given probability, p_c. If crossover is not implemented, the first of the two individuals is copied as child design. Otherwise, each child's ply orientation is a linear combination of the corresponding parent's ply orientations. An example of a flat crossover is given hereafter.

$$\begin{array}{llcl} \text{Parent 1:} & \theta_1^m & & \theta_2^m \\ \text{Parent 2:} & \theta_1^d & & \theta_2^d \\ \text{Child:} & \theta_1^c & & \theta_2^c \\ \text{where} & \theta_i^c & = & \alpha_i \theta_i^m + (1-\alpha_i)\theta_i^d, \ \alpha_i \in [0,1], \ i = 1,2. \end{array}$$

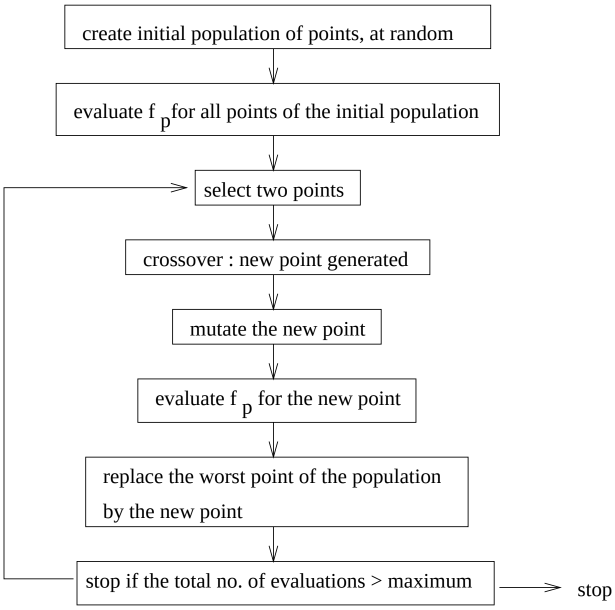

Figure 3: Flow Chart of a Steady-State Evolutionary Optimizer

After a child design has been created through crossover, a mutation operator is applied. Each design variable θ_i has a probability p_m of being changed by mutation. If it is decided to mutate θ_i, a new value is taken as a drawing of a random variable with a gaussian distribution centered on θ_i. The variance of the mutation is calculated such that, if θ_i is equal to $(\theta_i^{min} + \theta_i^{max})/2$, where θ_i^{min} and θ_i^{max} are the lower and upper bound of θ_i, respectively, then there are 95.5% chances that the new θ_i is between the bounds, i.e., the variance is equal to $(\theta_i^{min} - \theta_i^{max})^2/16$.

4.2 Stacking Sequence Optimization

The encoding scheme for the stacking sequence optimization represents a laminate cross-section with a series of angle identifiers. For example, a design point could be $(+\theta_2/+\theta_1/-\theta_1/-\theta_1/-\theta_2/+\theta_1)_s$.

Like in the continuous case, crossover is applied with a probability p_c. However, while exchanging substrings of selected points is the basis for most crossover operations, it is necessary here to adapt the crossover to our problem in order to preserve the same number of plies at $+\theta_1$, $-\theta_1$, $+\theta_2$, $-\theta_2$, in the parents and the child design. The proposed crossover, called order crossover, starts by choosing a breakpoint in the strings at random. Next the substring on the left of the breakpoint of the first parent design is copied onto the child design. Then, starting from the breakpoint and proceeding towards the right, ply angles from the second parent design that can be copied without changing the quotas of angles are copied. Locations where such a copy cannot occur are first left empty. They are filled during a second step, from the ply angles located on the right of the breakpoint of the first parent design. An example of order crossover is given hereafter where $\begin{smallmatrix}\vee\\\wedge\end{smallmatrix}$ designates the breakpoint:

Parent 1:	$+\theta_1$	$+\theta_2$	$+\theta_2$	$\begin{smallmatrix}\vee\\\wedge\end{smallmatrix}$	$-\theta_1$	$-\theta_2$	$-\theta_2$
Parent 2:	$-\theta_2$	$+\theta_1$	$-\theta_1$	$\begin{smallmatrix}\vee\\\wedge\end{smallmatrix}$	$-\theta_2$	$+\theta_2$	$+\theta_2$
step 1:	$+\theta_1$	$+\theta_2$	$+\theta_2$	$\begin{smallmatrix}\vee\\\wedge\end{smallmatrix}$	$-\theta_2$		
step 2, child:	$+\theta_1$	$+\theta_2$	$+\theta_2$	$\begin{smallmatrix}\vee\\\wedge\end{smallmatrix}$	$-\theta_2$	$-\theta_1$	$-\theta_2$

Contrary to the continuous case where the probability of mutation p_m concerns one design variable, mutation is applied here with a probability p_m per design (and not design variable). During mutation, two different ply angles are chosen at random, and their locations are permuted. An example of mutation for stacking sequence design is,

$$\begin{array}{lcccccc} \text{before mutation:} & +\theta_1 & +\boldsymbol{\theta_2} & +\theta_2 & -\theta_2 & -\boldsymbol{\theta_1} & -\theta_2 \\ \text{after mutation:} & +\theta_1 & -\boldsymbol{\theta_1} & +\theta_2 & -\theta_2 & +\boldsymbol{\theta_2} & -\theta_2 \end{array}$$

5 Applications to In-plane Design of Dimensionally stable plates

The objective is to find the thinnest, lowest α_x laminates that respect the constraints on in-plane properties given in the formulation (26). Two loading cases are being considered here.

Loading Case 1

$$F = \begin{bmatrix} F_x = 50000\ N \\ F_y = 100\ N \\ F_{xy} = 0\ N \end{bmatrix}$$

$$\begin{aligned} plate\ length &= 1\ m \\ plate\ width &= 0.1\ m \\ E_x^{min} &= 200\ GPa \\ E_y^{min} &= 5\ GPa \\ \beta_x^{allow} &= 10^{-9}\ /\ \%\ M \\ \varepsilon_x^{allow} &= 0.05\ \% \\ \varepsilon_y^{allow} &= 0.1\ \% \\ \alpha_x^{allow} &= 2.10^{-6}\ /\ ^\circ\ C \\ V_f &= 50\%,\ 60\% \end{aligned}$$

Loading Case 2

$$F = \begin{bmatrix} F_x = 20000\ N \\ F_y = 20000\ N \\ F_{xy} = 0\ N \end{bmatrix}$$

$$\begin{aligned} plate\ length &= 0.3\ m \\ plate\ width &= 0.3\ m \\ E_x^{min} &= 100\ GPa \\ E_y^{min} &= 10\ GPa \\ \beta_x^{allow} &= 10^{-1}\ /\ \%\ M \\ \varepsilon_x^{allow} &= 0.05\ \% \\ \varepsilon_y^{allow} &= 0.05\ \% \\ \alpha_x^{allow} &= 1.10^{-9}\ /\ ^\circ\ C \\ V_f &= 50\%,\ 60\% \end{aligned}$$

Any composite with a coefficient of thermal expansion higher in magnitude than α_x^{allow} will not be considered as an acceptable design. Loading case 1 emphasizes longitudinal properties and puts weak limits on transverse and shear properties. Loading case 1 is relevant to long structural components. On the contrary, longitudinal constraints are relaxed with loading case 2.

A high modulus carbon fiber (P75 from Amoco) is selected along with two matrices: an organic matrix (934 from Fiberite), and a light metal matrix (Magnesium alloy). P75-934 composite is chosen here because it is a well documented combination[17,18]. Basic characteristics of the material are given in Table 1.

5.1 P75/934 Organic Matrix In-plane Designs

Organic matrix composites are widely used in satellite structures. The combination of carbon fibers (with a sligthly negative CTE and a very high stiffness in one direction) and organic matrix (with a high positive CTE but a low stiffness) can produce various composites, including 0-CTE laminates. One of the drawbacks of this type of material is a tendency to absorb humidity on earth and desorb it in space, which induces a change in length according to the composite CME, β. To avoid this phenomenon, a stringent value of the allowable CME, β_x^{allow}, is set (10^{-9} / % M) for loading case 1.

Results of the thickness and angle optimization are compiled in Table 2. Constraints on ε_x are active and drive the laminate thickness. Constraints on ε_y and E_y are not active on that particular loading case and are not included in the table. High fiber volume fraction leads to thinner laminates because of higher ply stiffness. For load case 1, 9.2% of the weight can be saved by increasing the fiber volume fraction from 50% to 60%.

property	fiber P75	org. matrix 934	met. matrix Mg
ρ (ton/m^3)	1.9	1.3	1.8
E_L (GPa)	550.20	4.34	45.00
E_T (GPa)	9.52	4.34	45.00
G_{LT} (GPa)	6.90	1.59	17.30
ν_{LT}	0.20	0.37	0.33
α_L $(10^{-6}/\ ^\circ C)$	-1.35	43.92	26.00
α_T $(10^{-6}/\ ^\circ C)$	6.84	43.92	26.00
β_L $(10^{-6}/\ \%\ M)$	/	2000.0	/
β_T $(10^{-6}/\ \%\ M)$	/	2000.0	/

Table 1: Basic material properties.

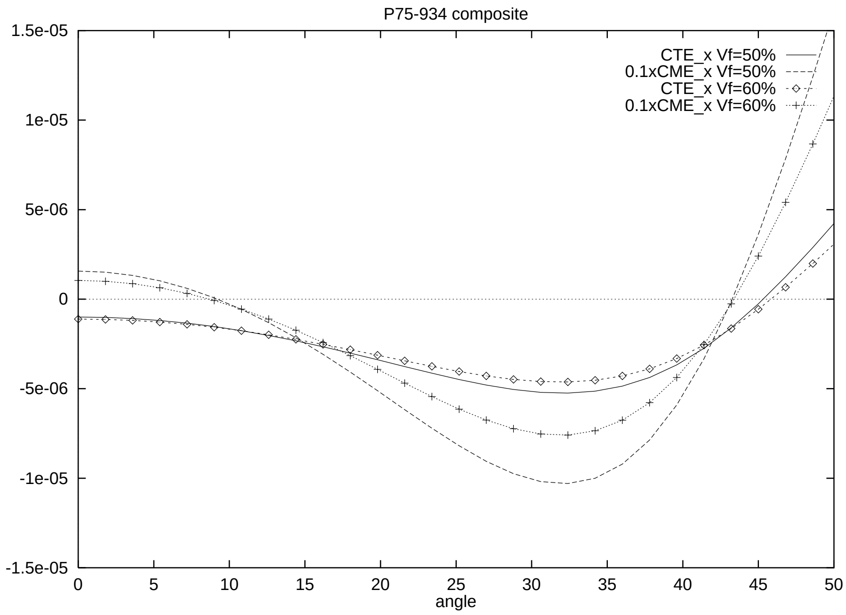

Figure 4: CTE_x and CME_x evolution

For loading case 1, constraints on β_x are active. They determine the ply angles. Optimal designs achieve low values of β_x, which is a stringent constraint. All designs have similar sligthly negative α_x. Figure 4 sheds a light on the first loading case optimal designs. Figure 4 shows α_x and β_x as a function of θ for a $(\pm\ \theta)_s$ composite (P75-934, $V_f = 60\ \%$). It is seen that α_x and β_x are not simultaneously zero. A value of θ around 10° yields a near-zero β_x and near $-2.\ 10^{-6}/\ ^\circ\ C$ α_x. Equivalent characteristics are observed in the OMC's optimal designs of Table 2.

For the second loading case, results of the thickness and angle optimization are compiled in Table 8 (this table also contains the results of the next sections where it is completely discussed). Constraints on β_x and E_x are much less stringent, thus allowing near-zero α_x laminates. Because longitudinal loading is slightly lower, the number of plies is also lower. Some fiber disorientation is needed to sustain y loading, while keeping a very low α_x. The active constraint with OMC's is E_x. Of course, because β_x is no more a constraint in that case, it takes substantial values with OMC's composites and would become a major contributor to long term dimensional instabilities if not controlled. On the other hand, strictly zero-α_x composites are obtained in that case, so that the overall longitudinal dimensional stability does not degrade too much.

5.2 P75-Mg Metal Matrix In-plane Design

We now consider a P75-Mg fiber-matrix composite. Metal matrix composites are good candidates for use in dimensionally stable structures because they are not subject to desorption and are good thermal conductors in comparison to organic matrix composites. One of their drawbacks is hysteresis and thermal ratchetting under large thermal cycles, due to residual stresses between fiber and matrix[19]. However, if thermal variations are reduced through structure thermal control, these phenomena are negligible, making the use of MMC's attractive. Results of thickness and angle optimization are given in table 3.

In general, MMC's have lower angle values θ_i's than OMC's, and have better dimensional stability characteristisc than OMC's: because moisture is not a preoccupation (the constraint on β_x is no longer active), α_x can be lowered to values close to zero. For the first loading case and $V_f = 50$ %, α_x is 0.50 $10^{-6}/°C$. It can be seen in that case that the active constraint is ε_x. If the ply angles are increased so as to lower α_x, E_x is reduced. The consequence would be an increase in ε_x, and then the violation of the related constraint. $\alpha_x = 0.50\ 10^{-6}/°C$ is not a physical limit for $V_f = 50\%$ MMC's in general, but it is a limit with 28 plies in the composite and the loads that have to be sustained. Lower α_x values could be reached at the expense of an increased laminate thickness.

When $V_f = 60$ % and for the first loading case, α_x is near zero, and the number of plies is 24. Composites are nearly unidirectional and stiffness is 21 % higher than with $V_f = 50\%$ MMC's. The comparison of OMC's and MMC's, $V_f = 60$ %, shows that MMC's best designs are stiffer, with virtually no thermal or hygral expansion. Eventhough MMC's density is higher than OMC's, MMC's optimal designs are 4% lighter than OMC's. This application illustrates the potential gains at using MMC's.

For the second loading case, results of the thickness and angle optimization are compiled in Table 8. Some disorientation is needed to sustain y loading, while keeping a very low α_x. It can be noticed in Table 8 that with $V_f = 50\%$, the number of plies is higher with MMC's than with their OMC's counterparts (26 against 16). The same result is obtained with $V_f = 60\%$. This is due to $\varepsilon_y^{allow} = 0.05$ % which is active on MMC's with a too low number of plies : near-zero α_x plates are in favor of quasi-unidirectional composites for MMC's, implying a low stiffness in y-direction. For OMC's, E_y of zero-α_x composites is much higher than with MMC's, allowing a lower number of plies, both with 50 and 60 % V_f. Because of a lower density and lower number of plies, OMC's designs are significantly ligther than MMC's solutions for loading case 2 : there is a 23 % weight reduction by changing the matrix from metal to organic in that case.

The results presented here show that the optimal material depends on the loading case: if longitudinal stiffness and low dimensional stability in the x direction is required (both α_x and β_x near zero), MMC's give the lowest weight solutions. But if both x and y directions are involved, OMC's solutions are lighter.

6 Stacking Sequence Optimization using Monte Carlo Analysis

6.1 Laminate Properties Distributions

The average and standard deviation of composite properties are estimated using a Monte Carlo technique. The standard deviation $\sigma(P)$ used in the calculation of the normally distributed P property is 2 % of the nominal value, at the exception of the standard deviation of ply angles $\sigma(\theta_i) = 1.8°$ (1.8 represents 2% of 90°). The tests reported in Figure 5 illustrate that $n_{MC} = 10000$ trials are sufficient to correctly describe laminate properties through their average standard deviations. It is shown that maximum errors (deviation) between properties standard deviations and their estimators are less than 2 % on the average of 5 tests with $n_{MC} = 10000$. Note that the reference standard deviations are based on 1 million trials.

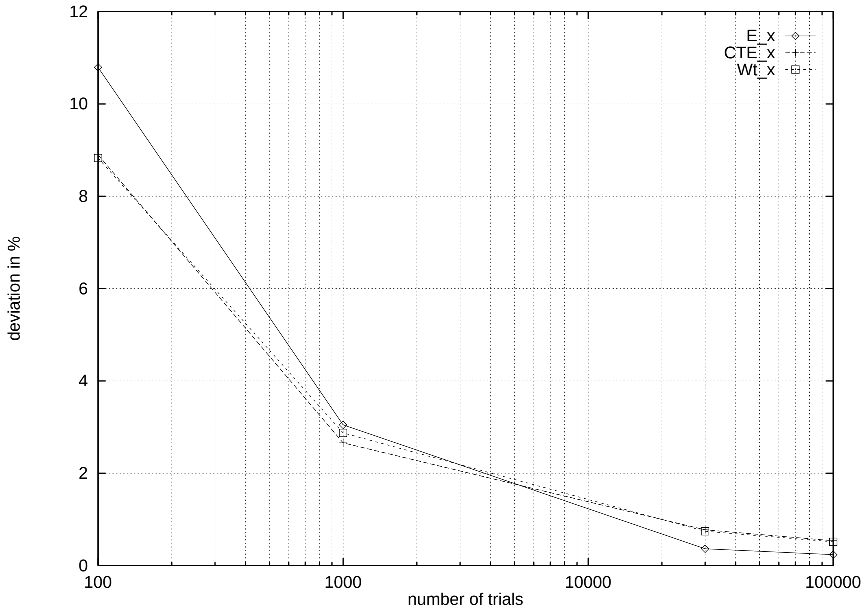

Figure 5: deviation between estimation and real value

In perfectly symmetric laminates, in-plane properties are not affected by the way the plies are stacked. This is no longer true with the perturbed unsymmetric laminates which have coupled in-plane and out-of-plane behaviors.

Different laminates based on 0°, 30° and −30° plies are compared in Table 4 in terms of nominal, and estimated average and standard deviation properties. The second sequence is shown twice so as to illustrate that 10000 is enough to estimate properties with a good accuracy. On the contrary, there is a strong effect of the stacking sequence on the standard deviation of the curvatures. For example, $\sigma(W_x^T)$ changes by 500% when the sequence $(0/30/-30)_s$ is replaced with $(-30/30/0)_s$.

Accordingly, out-of-plane optimizations for minimal deviations of curvatures such as described in Equations 27 and 28 are addressed next. The stacking order of a given number of plies is to be determined.

Before resorting to optimization, the plies obtained in section 5 are stacked using a rule of thumb: angles in minority are placed at regular intervals between angles in majority. This is a classical way of stacking plies to reduce delamination. For the loading case 1, results of the subsequent Monte Carlo analysis for longitudinal properties of OMC's are given in Table 5, and results for MMC's are given in Table 6. Comparing the standard deviations of OMC and MMC laminates, it is noticed that $\sigma(\alpha_x)$ is larger for MMC's than for OMC's. However, the opposite stands for $\sigma(W_x^T)$. Results for loading case 2 are given in Table 8. Because the number of plies in the laminate is lower, the number of possible composites is also lower. As for loading case 1, OMC's are less sensitive in α_x but more sensitive in deflection than MMC's. MMC's optimal laminates are stiffer and less likely to bend in changing environnements than OMC's.

6.2 Ply sequence optimization

For loading case 1, the problem formulation of equation (27) is used. Allowable values of the deviations, $\sigma(W_x^{d,allow})$, $\sigma(W_y^{d,allow})$, and $\sigma(W_{xy}^{d,allow})$, are set to 1.10^{-6} $/(m\ D)$, 1.10^{-5} $/(m\ D)$, and 1.10^{-5} $/(m\ D)$, respectively.

Optimal stacking sequences are given in Table 7 and compared to their traditional counterparts that were previously discussed. With an objective function based on $\sigma(W_x^T)$, 0° plies are located on the outside of the plate, while desoriented plies have the innermost positions. Such a result could be expected because, as it can be seen in Figure 6, the derivative of W_x is near zero with respect to change of fiber angle of a 0° ply on the outside. Moreover, the further 0° plies are from the laminate midplane, the more they affect the laminate W_x^T. Therefore, the stabilizing effect of 0° plies is maximized when they are on the outside of the laminate. Optimizing the stacking sequence of OMC's and MMC's plates reduces $\sigma(W_x^T)$ by as much as 40 %.

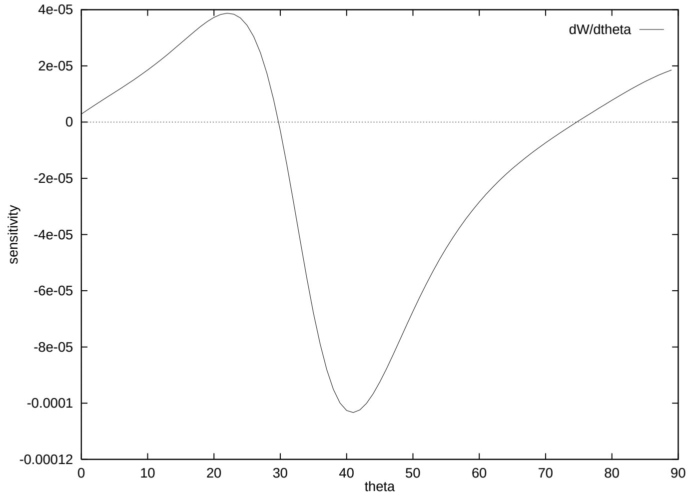

Figure 6: $\partial W_x/\partial\gamma$ at $\gamma = \theta$ for a $(\gamma/-\theta/(30)_4/(-30)_4/(-30)_4/(30)_4/-\theta/\theta)$ laminate

The problem formulation based on the deflection f is used for the second loading case, with $\sigma(f^{T,allow}) = 1.10^{-7} m/°C$. Optimal stacking sequences are given in Table 8 and compared to their traditional counterparts in terms of deflection dispersions. Stacking sequence optimization reduces by 10 % to 50 % the dispersion of deflection, thus significantly minimizing the risk of seeing deflected plates in service. After optimisation, OMC's are still more sensitive to thermal bending than MMC's.

7 Conclusions

A global approach to composite laminate design under hygral, thermal, and mechanical constraints has been proposed. First, the analysis is global since it starts with the micromechanical moduli of fibers and matrices, and since it accounts for manufacturing inaccuracies. Second, the optimization, performed mainly through evolutionary approaches, is global in scope. More precisely, in-plane deterministic design is performed, without loss of generality, on $[(\pm\theta_1)p/(\pm\theta_2)q]_s$ stacking sequences. The optimization of the ply angles θ_1 and θ_2 and the ply numbers p and q relies on a coupled heuristic enumerative scheme and an evolutionary algorithm. To decrease designs sensitivity to manufacturing inaccuracies, the stacking sequence is then optimized. The laminate stacking sequence combinatorial problem is solved by a second specialized evolutionary algorithm, in conjunction with a Monte Carlo analysis. Applications were provided for organic matrix and metal matrix composites.

The balance between dilatation and stiffness is in favor of MMC's when loads are essentially longitudinal. However, under combined longitudinal/transverse loads, OMC's remain better candidates, despite their sensitivity to moisture variations. It has been shown that substantial reductions of plate bending due to manufacturing inaccuracies can be obtained through stacking sequence optimization. In terms of bending, MMC's are slightly less sensitive to manufacturing errors than OMC's. The sensitivity in terms of other laminate properties are equivalent for MMC's and OMC's.

A continuation of the present work is to account for variations of composite properties with the temperature. The optimization problem decomposition performed here remains valid for varying temperatures. Furthermore, delamination criteria should be included in the analysis. On the experimental front, it is now necessary to test the composites optimized for reliable performance, and compare the results with traditional composites.

References

[1] Babel H. W., Shumate T. P., Thompson D. F., Microcrack Resistant structural Composite Tubes for Space Applications, *Sampe Journal*, May/June 1987, 43-48.

[2] Wolff E. G., Dimensional Stability of Structural Composites, *Metal Progress*, June 1979, 54-63.

[3] Jones R. M. , *Mechanics of Composite Materials*, McGraw-Hill, New York, 1975.

[4] Chamis C. C. , Simplified Composite Micromechanics Equations for Hygral, Thermal, and Mechanical Properties, *Sampe Quaterly*, April 1984, 14-23.

[5] Bowles D. E., Tompkins S. S. , Prediction of Coefficient of Thermal Expansion for Unidirectional Composites, *J. of Comp. Mat.*, **23**, April 1989, 370-387.

[6] Ishikawa T., Fukunaga H., and Ono K., Graphite-Epoxy Laminates with Almost Null Coefficient of Thermal Expansion under a Wide Range of Temperature, *J. of Material Science*, 1989, **24**, 2011-2017.

[7] Abernathy E., Mc Manus H. L., Effects of Material and Manufacturing Variations on Dimensionally Stable Composite Structures, *Proceedings of the Am. Soc. for Comp. 10th Technical Conf.*, Santa Monica, Oct 95.

[8] Mc Manus H. L., Probabilistic Methods for the Calculation of Laminate Properties, *J. of Reinforced Plastics and Comp.*, June 1993, **12**, 712-722.

[9] Holland, J. H., *Adaptation in Natural and Artificial Systems*, The University of Michigan Press, Ann Arbor, MI, 1975.

[10] Bäck, T., Hoffmeister, F., and Schwefel, H.-P., A Survey of Evolution Strategies, *Proceedings of the Fourth ICGA*, Morgan Kaufmann Publishers, Los Altos, CA, 1991, 2-9.

[11] Goldberg, D. E., *Genetic Algorithms in Search, Optimization and Machine Learning*, Addison-Wesley, Reading, MA, 1989.

[12] Le Riche, R., and Haftka, R. T., Improved Genetic Algorithm for Minimum Thickness Composite Laminate Design, *Composites Engineering*, 1995, **5**(2), 143-161.

[13] Kodiyalam S., Nagendra S., DeStefano J., Composite Sandwich Structure Optimization with Application to Satellite Components, *AIAA Journal*, March 1996, **34**(3), 614-621.

[14] Miki M., Material Design of Composite Laminates with Required In-Plane Elastic Properties, *ICCM-IV*, Tokyo, 1982, **2**, 1725-1731.

[15] *Evolutionary Algorithms in Engineering Applications*, D. Dasgupta and Z. Michalewicz, Eds., Springer Verlag Publ., ISBN 3-540-62021-4, March 1997.

[16] Radcliffe, N. J., *Genetic Neural Networks on MIMD Computers*, Ph.D. Dissertation, Univ. of Edinburgh, Edinburgh, UK, 1990.

[17] Blair, C., Zakrzewski, J., Mechanical and Thermophysical Properties for Dimensionally Stable High Modulus Graphite/Epoxy Composites, *SAMPE Quarterly*, April 1992, 2-7.

[18] Silverman, E. M., Sathoff, J. E., Forbes, W. C., Design of High Stiffness and low CTE Thermoplastic Composite Spacecraft Structures, *SAMPE Journal*, Sept-Oct. 89, **25**(5), 39-46.

[19] Wolff E. G., Min, B. K., Kural, M. H., Thermal Cycling of a Unidirectional graphite-magnesium Composite, *J. of Materials Science*, 1985, **20**, 1141-1149.

V_f (%)	**No. of plies**	**Mass** (Kg)	**Ply angles**	$\alpha_{\mathbf{x}}$ ($\mathbf{10^{-6}/^\circ C}$)	$\mathbf{E_x}$ (**GPa**)	ε_x %	β_x ($\mathbf{10^{-10}/\%M}$)
50.	32	0.64	$[(0^\circ)_{10}/(\pm 16.2^\circ)_3]_s$	-1.56	252.	0.0496	9.50
50.	32	0.64	$[(0^\circ)_8/(\pm 13.6^\circ)_4]_s$	-1.56	253.	0.0494	9.90
50.	32	0.64	$[(0^\circ)_4/(\pm 10.8^\circ)_6]_s$	-1.56	254.	0.0493	9.91
50.	32	0.64	$[(\pm 7.9^\circ)_6/(\pm 12.6^\circ)_2]_s$	-1.56	254.	0.0493	-4.85
50.	32	0.64	$[(0^\circ)_2/(\pm 9.9^\circ)_7]_s$	-1.56	254.	0.0492	9.44
50.	32	0.64	$[(\pm 11.2^\circ)_1/(\pm 8.9^\circ)_7]_s$	-1.56	254.	0.0492	9.36
50.	32	0.64	$[(\pm 9.2^\circ)_8]_s$	-1.56	254.	0.0492	9.99
60.	28	0.581	$[(0^\circ)_{10}/(\pm 18.1^\circ)_2]_s$	-1.54	304.	0.047	9.62
60.	28	0.581	$[(0^\circ)_8/(\pm 13.9^\circ)_3]_s$	-1.54	306.	0.0467	9.62
60.	28	0.581	$[(\pm 6.3^\circ)_4/(\pm 11.3^\circ)_3]_s$	-1.54	307.	0.0466	5.53
60.	28	0.581	$[(0^\circ)_4/(\pm 10.4^\circ)_5]_s$	-1.54	307.	0.0466	7.27
60.	28	0.581	$[(0^\circ)_2/(\pm 9.4^\circ)_6]_s$	-1.54	307.	0.0465	9.24
60.	28	0.581	$[(\pm 4.4^\circ)_6/(\pm 29.9^\circ)_1]_s$	-1.54	294.	0.0485	9.77
60.	28	0.581	$[(\pm 8.7^\circ)_7]_s$	-1.54	307.	0.0465	9.62

Table 2: Organic matrix composites solutions to the in-plane problem. Loading case 1

V_f (%)	**No. of plies**	**Mass** (Kg)	**Ply angles**	$\alpha_{\mathbf{x}}$ ($\mathbf{10^{-6}}/^\circ\mathbf{C}$)	$\mathbf{E_x}$ (**GPa**)	ε_x %	E_y (**GPa**)	ε_y %
50.	28	0.6475	$[(0°)_{10}/(\pm 13.5°)_2]_s$	0.50	285.	0.04999	12.31	−0.0260
50.	28	0.6475	$[(0°)_8/(\pm 10.9°)_3]_s$	0.50	285.	0.04999	12.33	−0.0263
50.	28	0.6475	$[(0°)_6/(\pm 9.4°)_4]_s$	0.50	285.	0.04999	12.34	−0.0264
50.	28	0.6475	$[(0°)_4/(\pm 8.4°)_5]_s$	0.50	285.	0.04999	12.52	−0.0265
50.	28	0.6475	$[(0°)_{12}/(\pm 19.8°)_1]_s$	0.51	285.	0.04999	12.24	−0.0252
50.	28	0.6475	$[(0°)_2/(\pm 7.6\circ)_6]_s$	0.50	285.	0.04999	12.35	−0.0265
50.	28	0.6475	$[(\pm 7.0°)_7]_s$	0.50	285.	0.04999	12.50	−0.0265
60.	24	0.558	$[(0°)_6/(\pm 4.5°)_3]_s$	0	345.	0.0483	11.59	−0.0132
60.	24	0.558	$[(0°)_{10}/(\pm 7.8°)_1]_s$	0	345.	0.0483	11.60	−0.0132
60.	24	0.558	$[(0°)_8/(\pm 5.5°)_2]_s$	0	345.	0.0483	11.60	−0.0132
60.	24	0.558	$[(0°)_4/(\pm 3.8°)_4]_s$	0	345.	0.0483	11.59	−0.0132
60.	24	0.558	$[(0°)_2/(\pm 3.4°)_5]_s$	0	345.	0.0483	11.59	−0.0132
60.	24	0.558	$[(\pm 3.1°)_6]_s$	0	345.	0.0483	11.59	−0.0132

Table 3: Metal matrix composites solutions to the in-plane problem. Loading case 1

Sequence	**Trial Numb.**	E_x^{nom} **(GPa)**	E_y^{nom} **(GPa)**	$\alpha_{\mathbf{x}}^{\mathbf{nom}}$ $(10^{-6}/^{\circ}C)$	$\alpha_{\mathbf{y}}^{\mathbf{nom}}$ $(10^{-6}/^{\circ}C)$	W_x^{Tnom}	$E_x \pm \sigma(E_x)$ **GPa**	$E_y \pm \sigma(E_y)$ **GPa**	$\alpha_x \pm \sigma(\alpha_x)$ $(10^{-6}/^{\circ}C)$	$\alpha_y \pm \sigma(\alpha_y)$ $(10^{-6}/^{\circ}C)$	$\sigma(W_x^T)$ $10^{-6}/(m\ ^{\circ}C))$
$[0/30./-30.]_s$	1	132.84	12.55	−2.556	9.678	0.	132.66(3.93)	12.55(0.45)	−2.555(0.049)	9.684(0.533)	0.9(95.9)
$[30/0./-30.]_s$	1	132.84	12.55	−2.556	9.678	0.	132.65(3.93)	12.54(0.44)	−2.554(0.049)	9.701(0.532)	−0.5(309.8)
$[30/0./-30.]_s$	2	132.84	12.55	−2.556	9.678	0.	132.73(3.97)	12.54(0.44)	−2.554(0.049)	9.701(0.531)	−2.3(312.9)
$[-30/30./0.]_s$	1	132.84	12.55	−2.556	9.678	0.	132.66(3.97)	12.54(0.44)	−2.554(0.050)	9.702(0.532)	4.8(511.7)

Table 4: Variations in properties of an OMC laminate ($V_f = 50\%$), with n=10000

V_f (%)	**No. of Plies**	**Ply angles**	$\sigma(\alpha_x)$ $(10^{-6}/^\circ C)$	$\sigma(E_x)$ (GPa)	$\sigma(W_x^T)$ $10^{-6}/(m\ ^\circ C))$	$\sigma(\beta_x)$ $(10^{-6}/\%M)$
50.	32	$[0/(0/16.2/0/-16.2/0)_3/0]_s$	0.041	7.5	24.	1.5
50.	32	$[(0/13.6/0/-13.6)_4]_s$	0.044	7.5	26.	1.7
50.	32	$[(\pm 10.8)/(0/10.8/-10.8)_4/(\pm 10.8)]_s$	0.047	7.5	28.	1.8
50.	32	$[(\pm 7.9)_2/-12.6/(\pm 7.9)_2/12.6/(\pm 7.9)_2]_s$	0.047	7.5	29.	1.9
50.	32	$[(\pm 9.9)_2/0/(\pm 9.9)_3/0/(\pm 9.9)_2]_s$	0.048	7.5	34.	1.9
50.	32	$[(\pm 8.9)_2/11.2/(\pm 8.9)_3/-11.2/(\pm 8.9)_2]_s$	0.048	7.5	34.	1.9
50.	32	$[(\pm 9.2)_8]_s$	0.048	7.5	32.	2.
60.	28	$[(0_2/-18.1/0_2/18.1)_2/0_2]_s$	0.036	8.3	22.	0.9
60.	28	$[((0_2)/(\pm 13.9))_3/(0_2)]_s$	0.039	8.3	26.	1.2
60.	28	$[(\pm 6.3)/(\pm 11.3)_3/(\pm 6.3)]_s$	0.043	8.3	30.	1.4
60.	28	$[(0/10.4/-10.4)_4/10.4/-10.4]_s$	0.042	8.4	34.	1.4
60.	28	$[(\pm 9.4)_2/0/(\pm 9.4)_2/0/(\pm 9.4)_2]_s$	0.043	8.4	34.	1.4
60.	28	$[\pm 4.6_2/29.9/\pm 4.6_2/-29.9/\pm 4.6_2]_s$	0.032	8	16.	0.7
60.	28	$[(\pm 8.7)_7]_s$	0.044	8.5	32.	1.4

Table 5: Standard deviations of organic matrix laminates properties. Loading case 1 without Sequence optimization.

V_f (%)	**Ply no.**	**Ply angles**	$\sigma(\alpha_x)$ $(10^{-6}/°C)$	$\sigma(E_x)$ (GPa)	$\sigma(W_x^T)$ $10^{-6}/(m\ °C))$
50	28	$[(0_2/-13.5/0_2/13.5)_2/0_2]_s$	0.11	7.4	12.
50	28	$[0/(0/10.9/0/-10.9)_3/0]_s$	0.11	7.5	15.
50	28	$[0/(0/9.4/-9.4)_4/0]_s$	0.11	7.5	16.
50	28	$[8/(0/8.4/-8.4)_4/-8]_s$	0.11	7.5	15.
50	28	$[0_4/19.8/0_4/-19.8]_s$	0.11	7.5	7.
50	28	$[\pm 7.6_2/0/\pm 7.6_2/0/\pm 7.6_2]_s$	0.11	7.5	16.
50	28	$[(\pm 7.0°)_7]_s$	0.11	7.5	16.
60	24	$[((0_2)/(\pm 4.5))_3]_s$	0.080	8.7	9.
60	24	$[0_4/7.8/0_4/-7.8/0_2]_s$	0.080	8.6	9.
60	24	$[(-5.5/0_2/5.5/0_2)_s]_s$	0.080	8.6	10.
60	24	$[(0/\pm 3.8)_4]_s$	0.080	8.6	9.
60	24	$[((\pm 3.4)_2/0)_s/(\pm 3.4)]_s$	0.080	8.6	10.
60	24	$[(\pm 3.1°)_6]_s$	0.080	9.2	8.

Table 6: Standard deviations of metal matrix laminates properties. Loading case 1 without Sequence optimization.

V_f (%)	**Matrix**	**Classical Seq.**	$\sigma(W_x^T)$	**Optim. Seq.**	$\sigma(W_x^T)$
50	934	$[(0/13.6/0/-13.6)_4]_s$	26.	$[0_8/(\pm 13.6)_4]_s$	15.
60	934	$[(\pm 4.6)_2/29.9/(\pm 4.6)_2/-29.9/(\pm 4.6)_2]_s$	16.	$[(\pm 4.6)_6/(\pm 29.9)]_s$	14.
50	Mg	$[0_4/19.8/0_4/-19.8/0_4]_s$	9.	$[0_{12}/(\pm 19.8)]_s$	4.
50	Mg	$[(\pm 7.6)_2/0/(\pm 7.6)_2/0/(\pm 7.6)_2]_s$	16.	$[0_2/(\pm 7.6)_6]_s$	15.
60	Mg	$[(0/\pm 3.8)_4]_s$	9.	$[(0)_4/(\pm 3.8)_4]_s$	7.

Table 7: Optimization of laminate sequences on $\sigma(W_x^T)$. Loading case 1

Loading Case 2	OMC $V_f = 50\%$	MMC $V_f = 50\%$	OMC $V_f = 60\%$	MMC $V_f = 60\%$
Number of plies	16	26	12	14
Mass (kg)	0.290	0.540	0.224	0.293
Optimized *Sequence*	$[-23.3/23.3_2/-23.3$ $/83.4_2/-83.4_2]_s$	$[37.7_3/0._2/37.7$ $/0./37.7/-37.7_5]_s$	$[\pm 15.2/\pm 87.7_2]_s$	$[47.7_2/-47.7_2/0._3]_s$
$E_x \pm \sigma(E_x)\ GPa$	100.5 ± 3.0	108.1 ± 2.1	101.2 ± 2.8	164.3 ± 3.7
$E_y \pm \sigma(E_y)\ GPa$	138.0 ± 3.8	29.7 ± 0.5	223.0 ± 5.8	59.2 ± 1.7
$\alpha_x \pm \sigma(\alpha_x)$ $(10^{-6}/°C)$	0.001 ± 0.065	0.000 ± 0.101	0.001 ± 0.062	0.001 ± 0.078
$\beta_x \pm \sigma(\beta_x)$ $(10^{-6}/(m\ °C))$	43.5 ± 2.2	0.	37.8 ± 2.0	0.
$\epsilon_x \pm \sigma(\epsilon_x)$ (%)	0.0282 ± 0.0008	-0.00249 ± 0.00028	0.0422 ± 0.0011	0.00736 ± 0.00041
$\epsilon_y \pm \sigma(\epsilon_y)$(%)	0.0192 ± 0.0005	0.0475 ± 0.0010	0.0181 ± 0.0005	0.0486 ± 0.0015
$\sigma(deflection)$ $(10^{-6}/(m\ °C))$	1.296	0.999	4.715	0.7763
Traditional *Sequence*	$[(23.3/83.4$ $/-83.4/-23.3)_2]_s$	$[(\pm 37.7/0.)_2/\pm 37.7]_s$	$[87.7/15.2/-87.7$ $/87.7/-15.2/-87.7]_s$	$[(47.7/0./-47.7$ $/0./47.7/0./-47.7]_s$
$E_x \pm \sigma(E_x)\ (GPa)$	100.6 ± 3.0	108.1 ± 2.1	101.0 ± 2.8	164.3 ± 3.7
$\alpha_x \pm \sigma(\alpha_x)$ $(10^{-6}/°C)$	0.002 ± 0.065	0.000 ± 0.101	0.001 ± 0.062	0.001 ± 0.078
$\sigma(deflection)$ $(10^{-6}/(m\ °C))$	2.262	1.102	9.896	1.01

Table 8: Loading case 2. Results of Angle and Stacking sequence optimization.